immunohistochemistry. Negative p53 nuclear immunoreaction (RSp53, Nichirei, Tokyo, Japan) and negative c-erbB-2 overexpression (Nichirei) by immunohistochemical staining were observed in this tumor. She received the neoadjuvant chemotherapy to completion and toxicities were tolerable. After the termination of chemotherapy, the tumor size was 2.5 × 2.5 cm by palpation (tumor shrinkage rate: 83%). The imaging examinations (MMG, US and CT) were also re-evaluated prior to surgery. The tumor sizes were 3.7 × 3.3 cm (60%) on MMG and 2.2 × 0.6 cm (92%) on CT (Fig. 1D). The tumor shadow remained but became vague on MMG. The low-density area disappeared on CT. However, on US, the lesion had completely disappeared and only a ductal structure was detected after the chemotherapy (Fig. 1E). In brief, a partial response was obtained clinically. A wide resection of the right breast was carried out 28 days after the termination of neoadjuvant chemotherapy. Histopathological examination revealed that the tumor had completely disappeared with negative lymph node metastasis (0/14). Only foamy changes with lymphocytic infiltration and stromal hyalinization could be observed in the resected specimen (Fig. 1F). The effect of neoadjuvant chemotherapy was therefore evaluated as a histologically complete response. Postoperative adjuvant chemotherapy consisting of two cycles of ADM plus TXT was given to the patient. She is currently disease free 6 months after surgery.

CASE 2

A 61-year-old postmenopausal woman with a left primary breast carcinoma (T3N0M0) received the above neoadjuvant chemotherapy. She had no past or family history of malignancies. Physical examination showed an ill-defined, stony-hard mass located in the upper inner quadrant of her left breast. The tumor size was 5.5 × 4.0 cm in diameter at the first consultation. MMG revealed an ill-defined tumor shadow without microcalcification in the left breast, the size of which was 3.3 × 2.8 cm in diameter. An irregular hypoechoic-tumorous lesion could be detected by US, the size of which was 3.1 × 3.0 cm in diameter. A lobulated tumorous lesion also could be detected on CT, the size of which was 3.0 × 2.5 cm in diameter. Core needle biopsy revealed an invasive ductal carcinoma of the left breast, histological grade 3. ER and PgR were both negative. Positive p53 nuclear immunoreaction but negative c-erbB-2 overexpression were observed in this tumor. She received the neoadjuvant chemotherapy to completion and toxicities were tolerable. After the termination of chemotherapy, the tumor size was 3.0 × 2.5 cm (66%). The imaging examinations (MMG, US and CT) were also re-evaluated prior to surgery. MMG illustrated a reduction in tumor size (2.1 × 1.6 cm: 64%). On US, whereas the lesion had been longer than wide before the chemotherapy, it was oval-shaped, horizontally oriented after the chemotherapy (1.5 × 0.9 cm: 85%). In addition, the internal echo changed from heterogeneous to homogeneous after the chemotherapy. Echogenic rim and bilateral retrotumoral shadowing were also evident after the chemotherapy. With regard to CT, the irregular tumorous lesion became smaller but still remained after the chemotherapy (2.0 × 1.5 cm: 60%). Therefore, a partial response was obtained clinically. A modified radical mastectomy (Auchincloss mode) was carried out 27 days after the termination of neoadjuvant chemotherapy. Histopathological examination revealed that the tumor had completely disappeared but without lymph node metastasis (0/13). With regard to the initial site of the tumor, only inflammatory changes with foamy macrophages and hemosiderin deposits could be observed in the resected specimen. The effect of neoadjuvant chemotherapy was therefore evaluated as a histologically complete response. Postoperative adjuvant chemotherapy consisting of two cycles of ADM plus TXT was given to the patient. She is currently disease free 8 months after surgery.

CASE 3

A 67-year-old postmenopausal woman with a right primary breast carcinoma (T3N0M0) received the above neoadjuvant chemotherapy. She had no past or family history of malignancies. Physical examination showed an ill-defined, stony-hard mass incompletely fixed to the skin, located in the upper outer quadrant of her right breast. The tumor size was 5.2 × 5.2 cm in diameter at the first consultation. MMG revealed an ill-defined spiculated tumor shadow with microcalcification in the right breast, the size of which was 3.0 × 3.0 cm in diameter (Fig. 2A). An irregular hypoechoic-tumorous lesion could be detected by US, the size of which was 4.0 × 4.0 cm in diameter. An irregular tumorous lesion also could be detected on CT, the size of which was 3.0 × 2.5 cm in diameter. Core needle biopsy revealed an invasive ductal carcinoma of the right breast, histological grade 3. ER and PgR were both negative. Positive p53 nuclear immunoreaction and positive c-erbB-2 overexpression were observed in this tumor. She received the neoadjuvant chemotherapy to completion and toxicities were tolerable. After the termination of chemotherapy, the tumor size was 2.5 × 2.5 cm (77%). The imaging examinations (MMG, US and CT) were also re-evaluated prior to surgery. On MMG, the lesion became smaller (2.0 × 1.5 cm: 67%) and the tumor spiculation became vague but microcalcification was unchanged (Fig. 2B). US illustrated a definite reduction in tumor size after the chemotherapy (1.5 × 0.9 cm: 92%). It could not be differentiated from fibrocystic changes, e.g. adenosis. With regard to CT, the irregular tumorous lesion became smaller but still remained after the chemotherapy (2.0 × 1.5 cm: 60%). Therefore, partial response was obtained clinically. A wide excision was carried out 27 days after the termination of neoadjuvant chemotherapy. Histopathological examination revealed that the right breast tumor had completely disappeared without lymph node metastasis (0/13). With regard to the initial site of the tumor, only fibrocystic changes with an aggregate of foamy and hemosiderin-laden macrophages and an inflammatory cell infiltrate could be observed in the resected specimen. The effect of neoadjuvant chemotherapy was therefore evaluated as a histologically complete response. Postoperative adjuvant

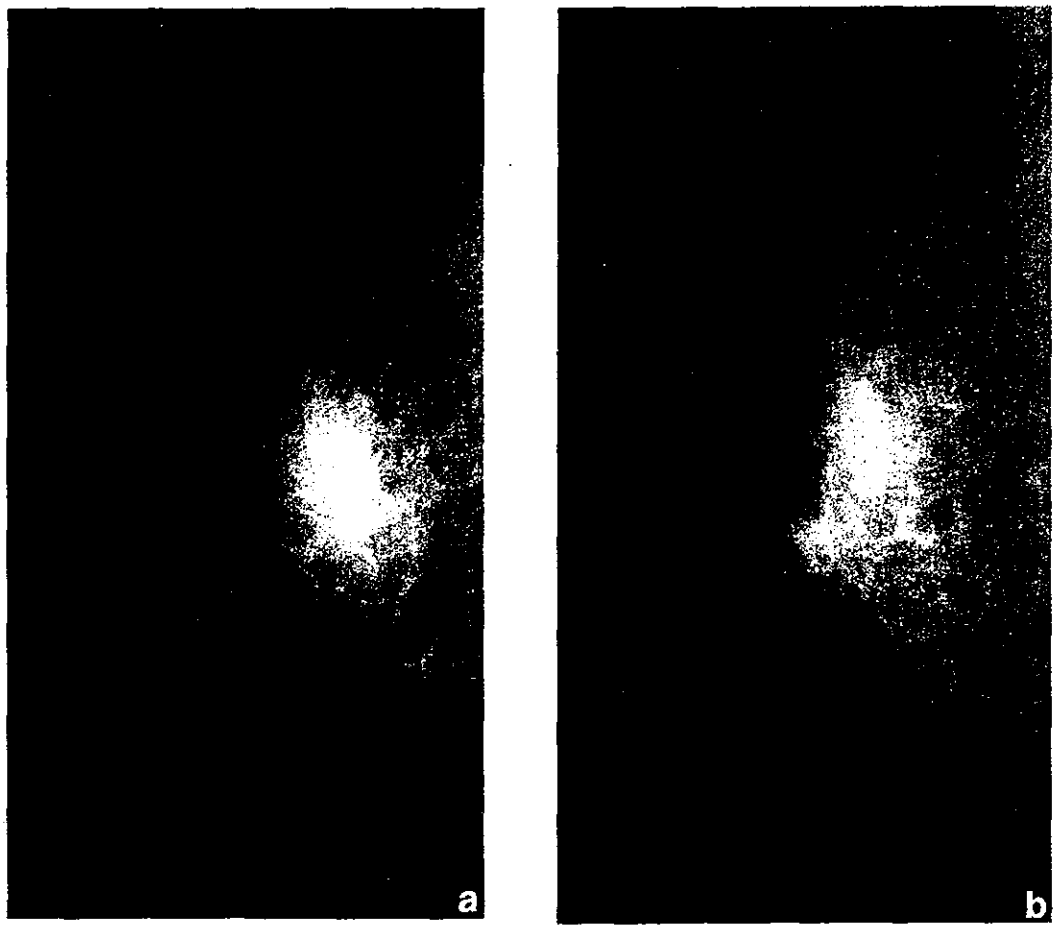

Figure 2. Case 3: a 67-year-old postmenopausal woman presented with a right primary breast carcinoma (T3N0M0). (A) MMG revealed an ill-defined spiculated tumor shadow with microcalcification, the size of which was 3.0 × 3.0 cm in diameter. (B) MMG indicated that the lesion had become smaller (2.0 × 1.5 cm) and the tumor spiculation had become vague, but microcalcification was unchanged.

chemotherapy consisting of two cycles of ADM plus TXT was given to the patient. She is currently disease free 10 months after surgery.

DISCUSSION

In these three cases with primary breast carcinoma after neoadjuvant chemotherapy, the resected specimen showed no microscopic evidence of residual cancer cells including an intraductal component in the primary lesions. There was histological evidence of tumor regression in each specimen. All patients were judged clinically as partial responders, because of the remaining tumorous lesions in the imaging examinations. However, these tumorous lesions could be related to the chemotherapy-induced fibrosis and tumor necrosis or the remaining fibrocystic changes.

Helvie et al. (4) documented that MMG was more sensitive than clinical examination in the prediction of residual carcinoma after chemotherapy. However, it was very difficult to evaluate the clinical meaning of the remaining microcalcifications after chemotherapy as in case 3. We previously reported that CT scanning was useful for evaluating histological tumor extension of breast carcinomas (5). Several authors have documented that contrast-enhanced magnetic resonance imaging could identify the residual disease in patients with breast cancer after neoadjuvant chemotherapy (6,7). Recently, the RECIST Working Group reported that US should not be used for the evaluation of cancer treatment (8). In this study, it was considered very difficult to estimate the extent of residual tumors accurately in patients with primary breast cancer after neoadjuvant chemotherapy by any type of imaging examination. In all specimens, chemotherapy-induced diffuse fibrosis and tumor necrosis were evident. The remaining tumorous lesion or microcalcification on the imaging examinations prior to surgery was not related to the cancerous changes but mainly to fibrosis or granulomatous changes due to tumor necrosis. These were the main reasons why imaging examinations tended to overestimate the residual tumor cells after chemotherapy.

The evaluation of the residual mass on the imaging examinations requires further studies. This will allow the selection of patients who may not need additional surgery.

References

1. Kuerer HM, Newman LA, Smith TL, Ames FC, Hunt KK, Dhingra K, et al. Clinical course of breast cancer patients with complete pathologic tumor and axillary lymph node response to doxorubicin-based neoadjuvant chemotherapy. *J Clin Oncol* 1999;17:460–9.
2. Wenzel C, Schmidinger M, Locker GJ, Taucher S, Gnant M, Jakesz R, et al. Clinical phase II evaluation of neoadjuvant, cytostatic combination chemotherapy with docetaxel and epidoxorubicin in female breast cancer patients (T1-4, N0-2, M0). *Wien Klin Wochenschr* 1999;111:843–50.
3. Nabholtz JM. Docetaxel plus doxorubicin-based combinations: the evidence of activity in breast cancer. *Semin Oncol* 1999;26:7–13.
4. Helvie MA, Joynt LK, Cody RL, Pierce LJ, Adler DD, Merajver SD. Locally advanced breast carcinoma: accuracy of mammography versus clinical examination in the prediction of residual disease after chemotherapy. *Radiology* 1996;198:327–32.
5. Akashi-Tanaka S, Fukutomi T, Miyakawa K, Uchiyama N, Tsuda H. Diagnostic value of contrast-enhanced computed tomography for diagnosing the intraductal component of breast cancer. *Breast Cancer Res Treat* 1998;49:79–86.
6. Tsuboi N, Ogawa Y, Inomata T, Yoshida D, Yoshida S, Moriki T. Changes in the findings of dynamic MRI by preoperative chemotherapy for patients with breast cancer of stage II and III: pathologic correlation. *Oncol Rep* 1999;6:727–32.
7. Esserman L, Hylton N, Yassa L, Barclay J, Frankel S, Sickles E. Utility of magnetic resonance imaging in the management of breast cancer: evidence for improved preoperative staging. *J Clin Oncol* 1999;17:110–9.
8. Therasse P, Arbuck SG, Eisenhauer EA, Wanders J, Kaplan RS, Rubinstein L, et al. New guidelines to evaluate the response to treatment in solid tumors. *J Natl Cancer Inst* 2000;92(3):205–16.

Int. J. Cancer (Radiat. Oncol. Invest): 96, 66-73 (2001)

Publication of the International Union Against Cancer

Accuracy of Contrast-Enhanced Computed Tomography in the Prediction of Residual Breast Cancer after Neoadjuvant Chemotherapy

Sadako Akashi-Tanaka, M.D.,[1]* Takashi Fukutomi, M.D.,[1]
Toru Watanabe, M.D.,[2] Noriyuki Katsumata, M.D.,[2]
Takeshi Nanasawa, M.D.,[1] Kaneyuki Matsuo, M.D.,[1]
Kunihisa Miyakawa, M.D.,[3] and Hitoshi Tsuda, M.D.[4]
[1]*Division of Surgical Oncology, National Cancer Center Hospital, Tokyo, Japan*
[2]*Division of Medical Oncology, National Cancer Center Hospital, Tokyo, Japan*
[3]*Department of Diagnostic Radiology, National Cancer Center Hospital, Tokyo, Japan*
[4]*Pathology Division, National Cancer Center Research Institute, Tokyo, Japan*

SUMMARY **Determination of the extent of residual disease after neoadjuvant chemotherapy is sometimes inaccurate by conventional diagnostic methods. The purpose of this study was to evaluate the accuracy of contrast-enhanced computed tomography (CE-CT) in depicting the extent of residual carcinomas. Fifty-seven patients with breast carcinomas of 3 cm diameter or more received neoadjuvant chemotherapy with four cycles of AT (doxorubicin and docetaxel). Before surgery, the patients underwent clinical examination, mammogram (MMG), ultrasonography (US), and CE-CT. Thirteen patients were not evaluated by CE-CT before surgery. Enhancement patterns on CE-CT were classified into multiple spots, tumor and spots, solid tumor type, and no enhancement. When all types of cancers were included in the analysis, clinical examination showed the best correlation with the pathology of the extent of residual carcinomas. However, except in invasive lobular carcinoma (ILC) and inflammatory breast carcinoma (IBC), CE-CT showed the best correlation ($R^{\wedge 2} = 0.537$). More than half of the residual microcalcifications on MMG after neoadjuvant chemotherapy suggested residual viable tumor. In conclusion, CE-CT is the most accurate noninvasive technique for identifying the extent of the residual carcinoma after neoadjuvant chemotherapy if cases of IBC and ILC are excluded.** *Int. J. Cancer (Radiat. Oncol. Invest.) 96, 66–73 (2001).* **© 2001 Wiley-Liss, Inc.**

Key words: CT scan; breast cancer; neoadjuvant chemotherapy; breast-conserving surgery; diagnostic x-ray

INTRODUCTION

The use of neoadjuvant chemotherapy has been extended to operable breast cancer. A large randomized clinical trial has confirmed the efficacy of neoadjuvant chemotherapy in downstaging and permitting lumpectomies [1], although no survival advantage has been demonstrated. The dilemma in the management of breast cancer after neoadjuvant chemotherapy is in defining the extent of residual disease so that appropriate surgery may be undertaken. Some reports have suggested that physical examination and mammogram (MMG) are complementary in the assessment of primary tumor response [2,3], whereas other reports have concluded that sonographic measurements correlate best with pathological findings [4]. Clinical measurements of breast masses are often inaccurate, and substantial

*Correspondence to: Sadako Akashi-Tanaka, M.D., Department of Surgical Oncology, National Cancer Center Hospital, 1-1 Tsukiji 5-chome, Chuo-ku, Tokyo 104-0045, Japan. Phone: 3-3542-2511; Fax: 3-3545-3567; E-mail: sakashi@gan2.ncc.go.jp

Received 02 May 2000; Revised 31 October 2000; Accepted 6 November 2000. Published online 6 February 2001.

interindividual variation exists among examiners [5]. Chemotherapy-induced fibrosis impairs evaluation of residual tumors by means of clinical examination, MMG, and ultrasonography (US) [6].

We have reported excellent resúlts with contrast-enhanced computed tomography (CE-CT) in demonstrating the extensive intraductal component (EIC) and small invasive foci of breast carcinoma [7,8]. The purpose of this study was to evaluate the accuracy of CE-CT in depicting the extent of residual carcinomas after neoadjuvant chemotherapy.

MATERIALS AND METHODS

Patients

Fifty-seven patients with breast carcinoma of 3 cm diameter or more underwent neoadjuvant chemotherapy at our hospital from May 1998 to January 2000. The treatment protocol comprised four cycles of AT (doxorubicin, docetaxel) at a dose of 50 and 60 mg/m^2 with a cycle length of 21 days, followed by mastectomy or breast-conserving surgery. The eligible women had initial pathologic confirmation of breast carcinoma by core needle biopsy. Complete staging in the form of chest x-ray, liver ultrasonography, and bone scan was performed in all patients at the beginning of neoadjuvant treatment. After the final chemotherapy cycle, patients were evaluated by palpation and imaging, including MMG, US, and CE-CT. Thirteen patients were not evaluated by CE-CT before surgery.

Imaging Examinations

Helical CT scanning was performed using an X-Vigor (Toshiba, Japan) at 300 mA. The patients underwent one single spiral acquisition during deep inspiratory apnea for up to 30 sec in the supine position. The first step was identification of the main tumor by a non-contrast-enhanced CT scan from the cranial end of the sternum to the inframammary fold. Subsequently, enhanced zoomed scanning was planned from 50 mm above to 50 mm below the main tumor with a collimation of 5 mm and a pitch of 1 mm. One hundred milliliters of non-ionic contrast material (300 mg I/g) was injected at a rate of 2 ml/sec. The time between the administration of the bolus injection of contrast material and the initiation of scanning was 60 sec. The reconstruction interval was 5 mm.

For mammographic examination, a Mammomat 3000 (Siemens, Germany) was used. In addition to standard oblique and cranio-caudal projections, cranio-caudal or medio-lateral spot views (5 cm in diameter) without magnification were obtained in most cases. Whole-breast US was performed using a model SSA340A device (Toshiba) with an annular array transducer. Tumor diameters were measured in a transverse direction with all modalities in this study. We measured the extent of tumor shadows and microcalcifications evident on MMG [9], low echoic masses and irregularly dilated ducts on US [10], and enhanced masses and spotty nodular enhancements on CE-CT [8] to determine the extent of residual carcinomas.

Surgical specimens were sectioned at about 7–10-mm intervals in a transverse direction and analyzed by breast pathologists. The classification of response to neoadjuvant chemotherapy was defined according to the general rules for clinical and pathological recording of breast cancer [11]: grade 0, no response was observed; grade 1a, slight degenerative change in any range of area or severe degenerative change in one-third of cancerous cells was observed; grade 1b, severe degenerative change was observed in one-third to two-thirds of cancerous cells; grade 2, more than two-thirds of cancerous cells were degenerated; and grade 3, complete response, no cancerous cells were observed. These slices were compared with the area of CE-CT abnormality and with the cranio-caudal view of the MMG and US.

Table 1. Patient and Tumor Characteristics at Entry to Neoadjuvant Chemotherapy*

Parameter	No. of patients (no. evaluated by CE-CT)
Total	57 (42)
Median age in years	48
(range)	(29–69)
Primary tumor status	
T2	21 (20)
T3	16 (12)
T4a–c	14 (8)
T4d	6 (2)
Pathology	
Invasive ductal carcinoma	50 (35)
Invasive lobular carcinoma	5 (5)
Other	2 (2)

CE-CT = contrast-enhanced computed tomography.

RESULTS

At the time of this evaluation, 57 patients had finished chemotherapy. Fifty-five patients underwent surgery, one rejected surgery, and another ended chemotherapy in the second cycle because of progressive disease. Forty-two patients were evaluated by CE-CT before surgery. The characteristics at entry of this protocol of 57 patients are shown in Table 1. Overall clinical response rate by clinical examination (cCR +cPR) was 86.0% (49/57). Six

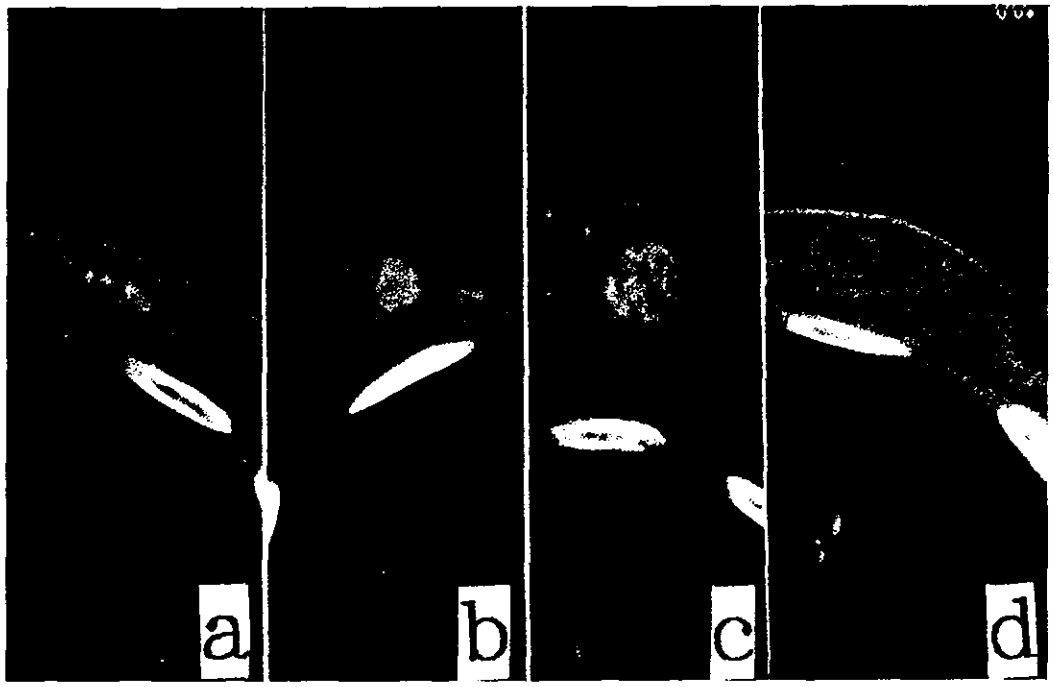

Fig. 1. Examples of patterns of enhancement on contrast-enhanced computed tomography (CE-CT): (**a**) multiple spots type, (**b**) tumor and spots type, (**c**) solid tumor type, and (**d**) no enhancement.

patients (10.5%) achieved cCR, and 43 patients (75.4%) achieved cPR. Three tumors (3/55: 5.5%) displayed pathological grade 3 response, 18 (18/55: 32.7%) grade 2 response, 24 (24/55: 43.6%) grade 1b response, 9 (9/55: 16.4%) grade 1a response, and 1 (1.8%) displayed no response.

The patterns of enhanced lesions on CE-CT were classified into multiple spots, tumor and spots, solid tumor type, and no enhancement, as shown in Figure 1. The correlations between residual invasive and/or intraductal components and enhanced patterns are shown in Table 2. The multiple spots type was related to residual intraductal components. Although no residual cancer was present, two patients appeared to have solid tumors by CE-CT as well as by MMG and US because of a cyst with fibrosis and an adenosis adjacent to the primary cancer. Cases that showed no enhancement on CE-CT included one case of inflammatory carcinoma (IBC), two cases of invasive lobular carcinoma (ILC), three cases of tiny residual cancer (under 3 mm), and one case of pathological complete response.

The correlations between the clinical, sonographic, mammographic, and CT measurements with pathological measurement of residual tumor diameters are presented in Figures 2–5. The coefficients of correlation between pathological size and types of evaluation were 0.333, 0.311, 0.156, and 0.181, respectively (Table 3). The discrepancies in size in CE-CT for IBC and ILC were marked, as shown in Figure 5. If cases of ILC and IBC are excluded, then CE-CT showed the best correlation ($r^2 = 0.537$) with pathology of the extent of residual carcinomas.

After neoadjuvant chemotherapy, widespread calcifications on MMG could be seen in 13 patients, even if the tumor shadows had disappeared or become smaller on MMG. In five cases, viable residual cancer cells were present within almost the same extent of microcalcification. In eight cases, the extent of the tumors was much smaller than that of the microcalcifications on MMG and almost equal to that of CE-CT enhancement (Fig. 6).

DISCUSSION

Neoadjuvant chemotherapy permits more breast-conserving surgery, particularly in patients with large tumors [1]. With the newer chemotherapeutic agents, the response of breast carcinoma to preoperative chemotherapy may be dramatic. In some patients, the tumor is no longer visible on either MMG or US. Thus, the rate of ipsilateral breast tumor recurrence was greater in women who were initially candidates for a mastectomy but who subsequently underwent a lumpectomy than in those who were initially considered candidates for lumpectomy [1]. This suggests that a more accurate modality for evaluating residual tumors is needed.

To our knowledge, only one study has been reported that evaluated CT for assessing the effect

Table 2. Relationship Between Enhancement Patterns on CE-CT and Residual Cancer Components*

Type	Residual cancer component				
	DCIS or mainly intraductal[a]	Invasive ductal cancer with EIC	Invasive carcinoma	No. tumor	Total
Multiple spots	2	1			3
Tumor and spots	2	3	5		10
Solid tumor	2	4	14	2	22
No enhancement	1		5	1	7
Total	7	8	24	3	42

*CE-CT = contrast-enhanced computed tomography; DCIS = ductal carcinoma in situ; EIC = extensive intraductal component.
[a]Tumors in which more than 80% of the area was occupied by an intraductal component.

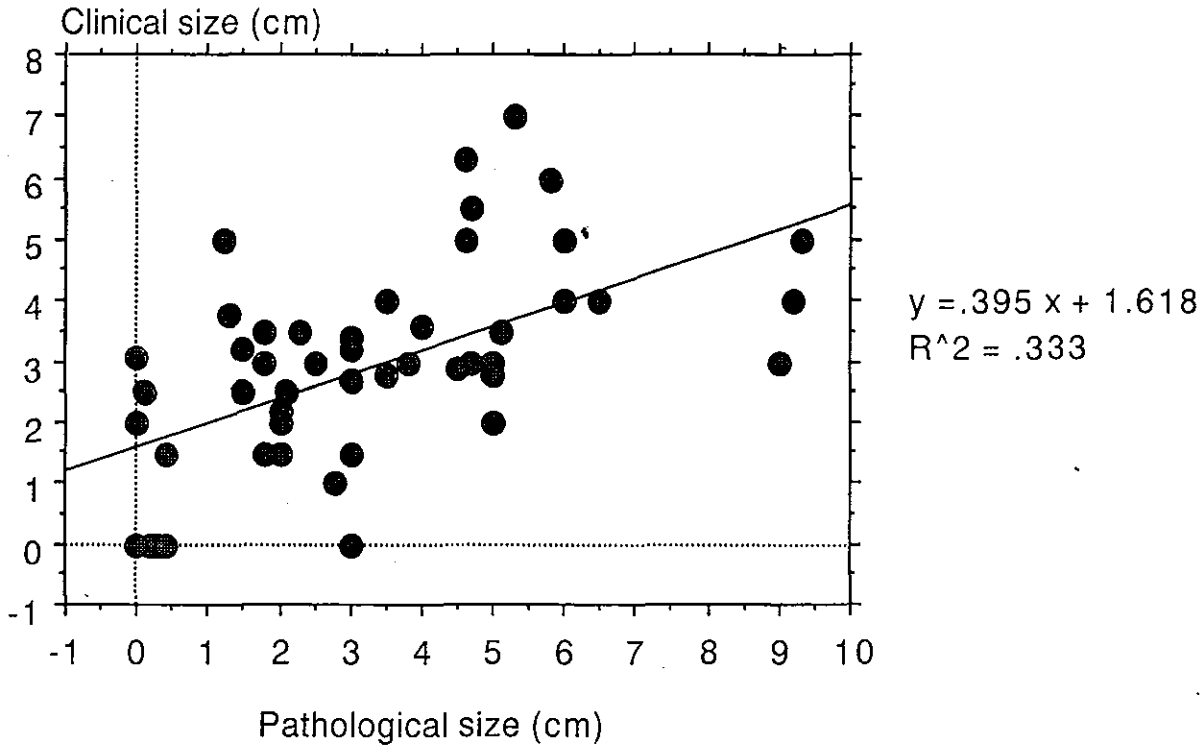

Fig. 2. Correlation between clinical sizes and pathological measurements.

of chemotherapy [12]. Lluch et al. [12] performed CT examinations in 44 patients and concluded that CT was a sensitive and accurate noninvasive technique for assessing axillary involvement after neoadjuvant chemotherapy in breast cancer and that clinical examination remains the best method for estimating primary tumor size.

We have reported excellent results of CE-CT in detecting EIC and small invasive foci and the usefulness of CE-CT in determining the extent of resection when performing CT of the breast [7,8]. In this study also, CE-CT depicted residual cancerous lesions after preoperative chemotherapy most accurately among conventional diagnostic methods. As shown in Figure 5, almost all the dots except for those of IBC and ILC fell between $y = x - 2$ and $y = x + 2$. The precise location of enhancement can be estimated easily by the combination of the number of slices from the nipple cephalocaudally and the distance from the sternum or the nipple transversally. This may suggest that a wide excision determined by CE-CT with 2 cm of free margin is the optimal excision extent.

Some studies using magnetic resonance imaging (MRI) reported its potential role in defining the extent of residual disease [13–16]. The pharmacokinetics of CT iodinated contrast agents is similar to that of nonselective Gd-chelates used as intrave-

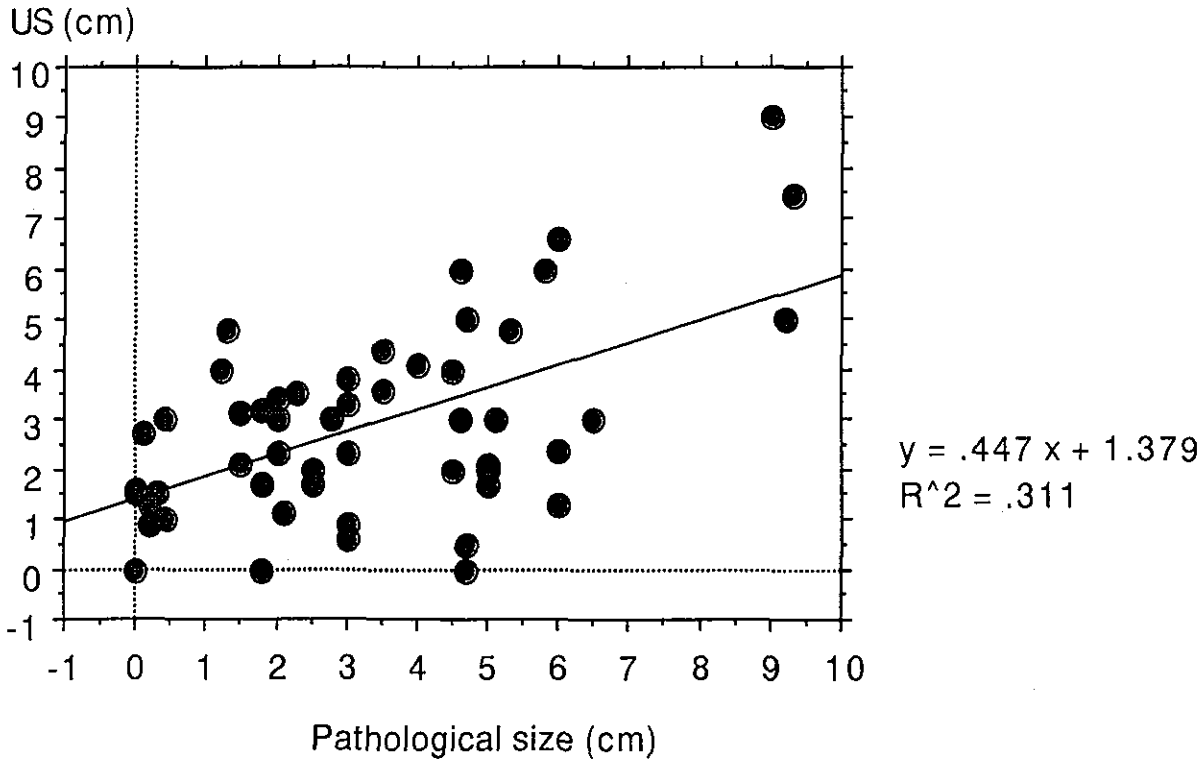

Fig. 3. Correlation between ultrasonographic (US) sizes and pathological measurements.

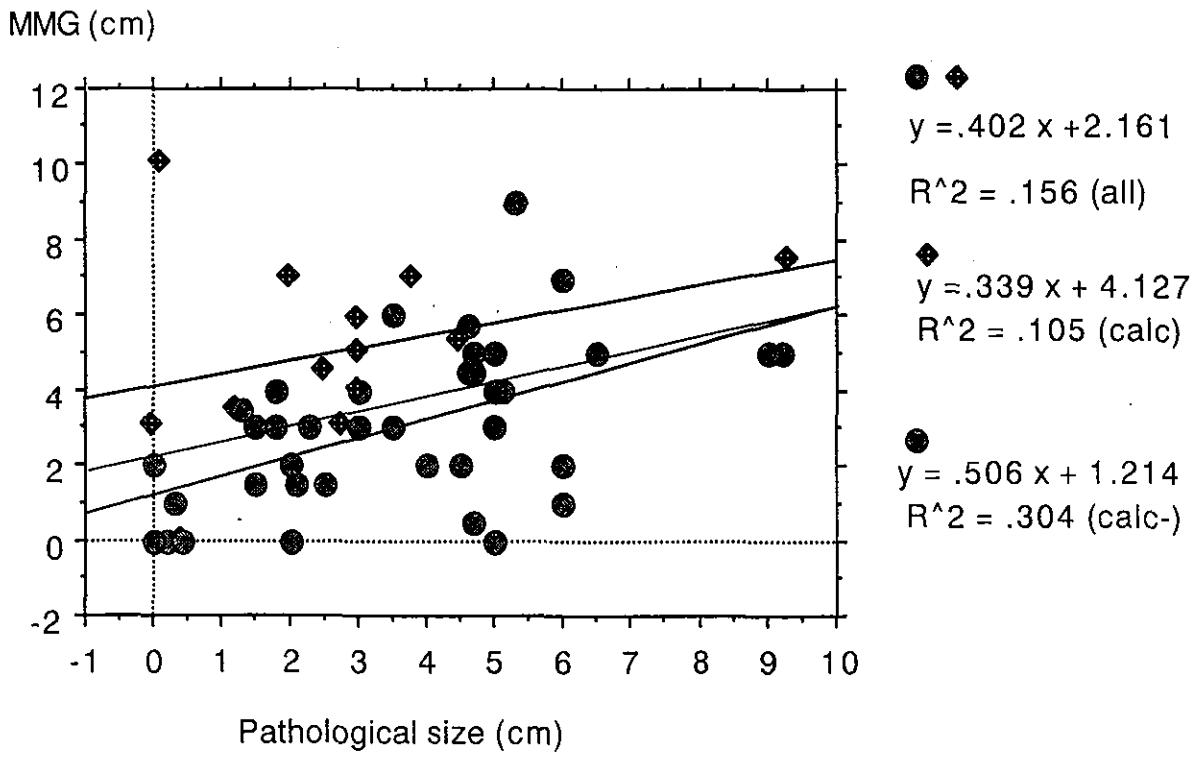

Fig. 4. Correlation between mammographic (MMG) sizes and pathological measurements. Circles, tumor without microcalcifications; diamonds, tumor with microcalcifications.

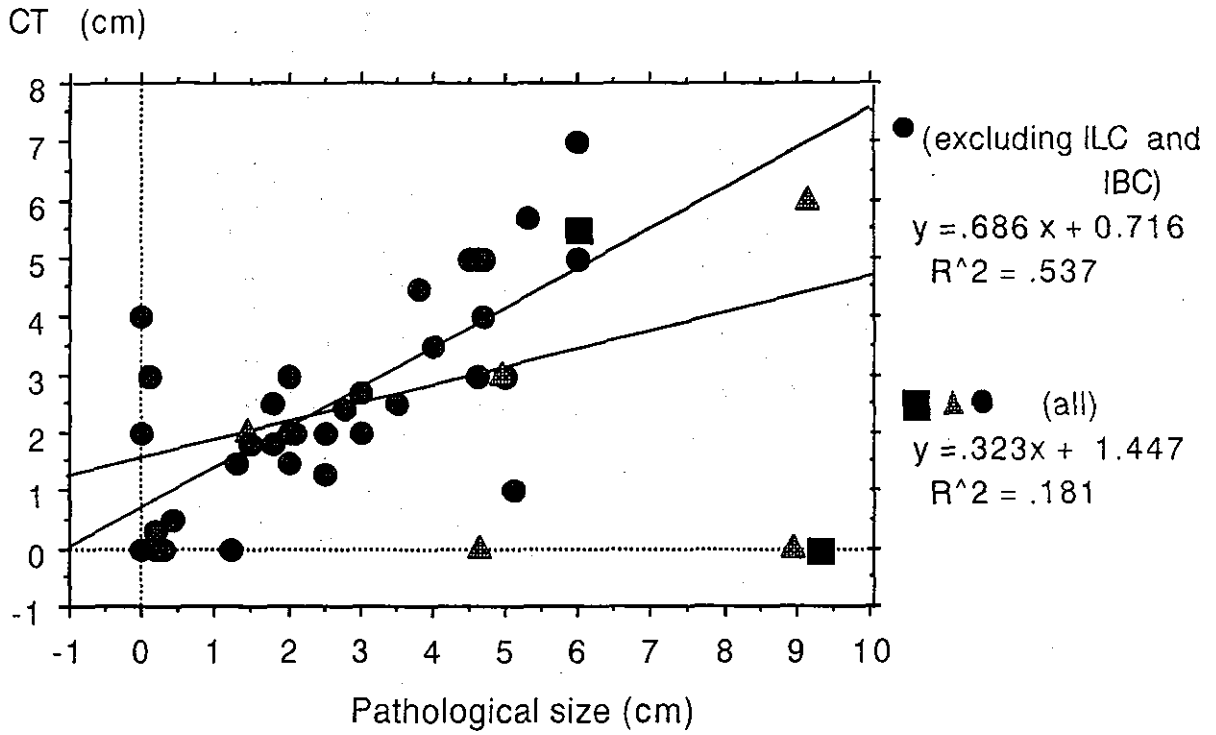

Fig. 5. Correlation between sizes determined by contrast-enhanced computed tomography (CE-CT) and pathological measurements. Squares, inflammatory breast carcinoma (IBC); triangles, invasive lobular carcinoma (ILC); circles, others.

Table 3. Spearman's Rank Correlation Coefficients ($R^{\wedge 2}$) of Noninvasive Measurements Obtained after NACT (before Surgery) Compared with Pathological Measurements*

Examination	$R^{\wedge 2}$
Clinical examination	0.333
Ultrasonography	0.311
Mammography	0.156
Cases without microcalcifications	0.304
CE-CT	0.181
Cases other than IBC and ILC	0.537

*CE-CT = contrast-enhanced computed tomography; IBC = inflammatory breast cancer; ILC = invasive lobular carcinoma; NACT = neoadjuvant chemotherapy.

nous MR contrast agents, characterized by intravascular and interstitial distribution [17]. MRI has better tissue resolution than do the other imaging techniques. Helical CT has some advantages over MRI, as follows: 1) the CE-CT examination takes only about 5 min; 2) CE-CT breast images are obtained in the supine position used during surgery, thus providing precise information about the extent of cancerous tissue in the breast; in contrast, in most previous studies of MRI, patients were examined in the prone position to minimize motion of the breast during breathing—the breast can shift and change its shape easily; 3) image quality of MRI depends greatly on the performance of the machine employed and requires complicated technical parameters; 4) CE-CT has a higher spatial resolution; 5) CE-CT is less expensive; and 6) MRI contraindications may be present, such as patients with a pacemaker or serious claustrophobic syndrome [18].

It is widely accepted that the presence of microcalcifications on MMG suggests the presence of EIC [9]. We might consider mastectomy safe when the widespread microcalcifications are demonstrated on MMG after neoadjuvant chemotherapy. However, more than half of these microcalcifications did not indicate residual tumor. Fortunately, they did not demonstrate enhancement on CE-CT, and we could distinguish the presence of widespread residual tumor from its absence. After this experience, we could reduce the extent of resection of the breast according to CE-CT. The microcalcifications remaining after neoadjuvant chemotherapy should be treated carefully.

It has been reported that quantitative positron emission tomographic (PET) scanning of tumor glucose metabolism with the glucose analog 2-^{18}F-fluoro-2-deoxy-D-glucose (FDG) has substantial potential as a research and clinical tool for monitoring the efficacy of chemohormonotherapy [19].

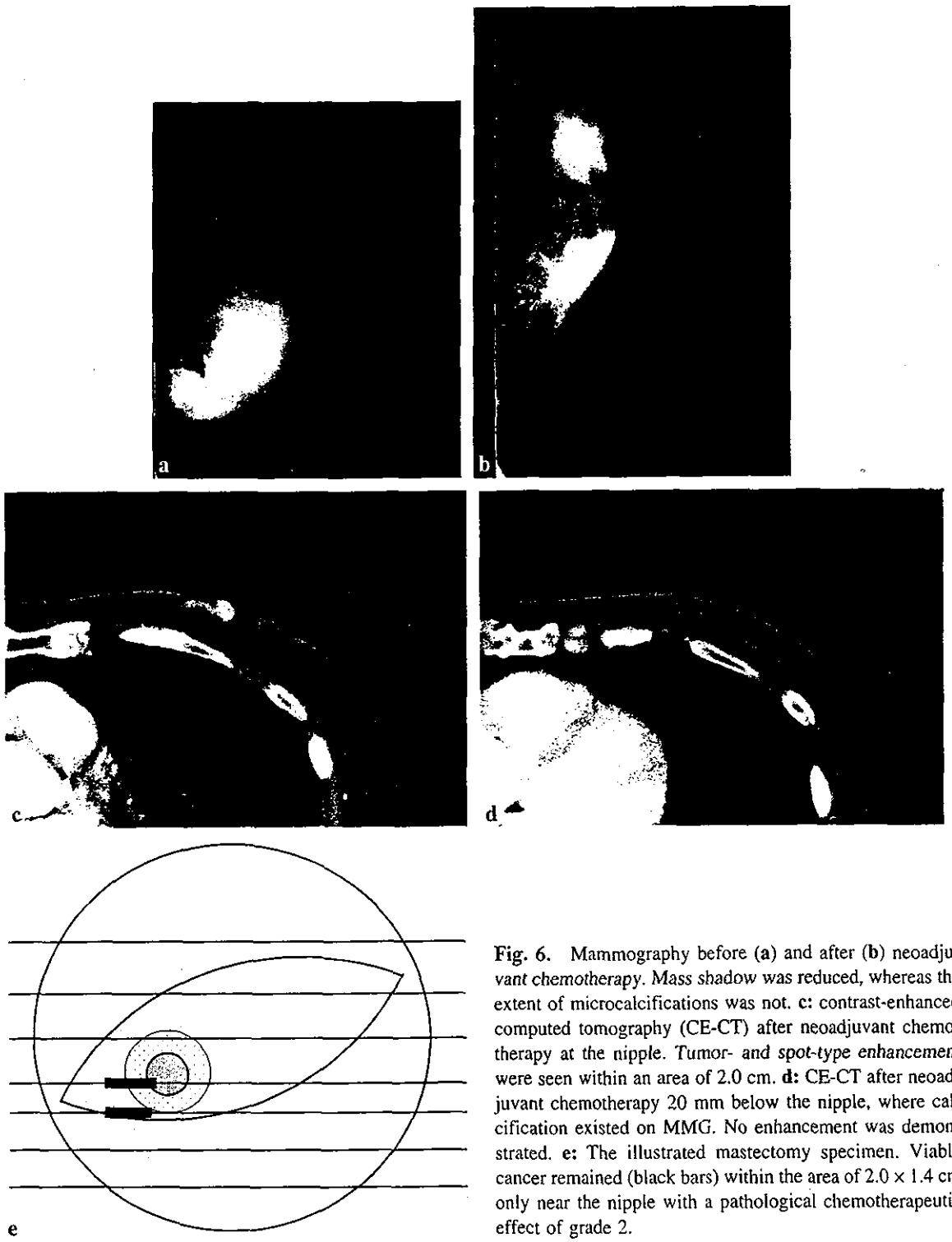

Fig. 6. Mammography before (**a**) and after (**b**) neoadjuvant chemotherapy. Mass shadow was reduced, whereas the extent of microcalcifications was not. **c:** contrast-enhanced computed tomography (CE-CT) after neoadjuvant chemotherapy at the nipple. Tumor- and spot-type enhancement were seen within an area of 2.0 cm. **d:** CE-CT after neoadjuvant chemotherapy 20 mm below the nipple, where calcification existed on MMG. No enhancement was demonstrated. **e:** The illustrated mastectomy specimen. Viable cancer remained (black bars) within the area of 2.0 x 1.4 cm only near the nipple with a pathological chemotherapeutic effect of grade 2.

PET demonstrated a decline in FDG uptake in patients responsive to treatment, whereas no significant decline in FDG uptake was seen in the non-responding patients examined after the initiation of treatment. We will evaluate whether the intensity of enhancement correlated with angiogenesis [20] might be a predictor of response to chemotherapy.

In conclusion, CE-CT is useful for identifying the extent of residual carcinoma after neoadjuvant chemotherapy. However, IBC and ILC should be treated carefully because they are not illustrated accurately by CE-CT.

REFERENCES

1. Fisher B, Bryant J, Wolmark N, Mamounas E, Brown A. Effect of preoperative chemotherapy on the outo-

come of women with operative breast cancer. J Clin Oncol 1998;16:2672–2685.
2. Dershaw DD, Drossman S, Liberman L, Abramson A. Assessment of response to therapy of primary breast cancer by mammography and physical examination. Cancer 1994;75:2093–2098.
3. Segel M, Paulus DD, Hortobagyi GN. Advanced primary breast cancer: assessment at mammography of response to induction chemotherapy. Radiology 1988; 169:49–54.
4. Herrada J, Iyer RB, Atkinson EN, Sneige N, Buzdar AU, Hortobagyi GN. Relative value of physical examination, mammography, and breast sonography in evaluating the size of the primary tumor and regional lymph node metastases in women receiving neoadjuvant chemothrapy for locally advanced breast carcinoma. Clin Cancer Res 1997;3:1565–1569.
5. Hortobagyi GN, Singletary SE, Strom EA. Treatment of locally advanced and inflammatory breast cancer. In: Harris J, Lippman ME, Morrow M, Osborne CK (eds). Diseases of the Breast, 2nd ed. Philadelphia: Lippincott Williams & Wilkins; 1999. p 647.
6. Singletary S, McNeese M, Hortobagyi GN. Feasibility of breast-conservation chemotherapy for locally advanced breast carcinoma. Cancer 1992;69:2849–2852.
7. Akashi-Tanaka S, Fukutomi T, Miyakawa K, Tsuda H. Diagnostic value of enhanced computed tomography in the detection of the widely spreading intraductal component of breast cancer: case reports. Breast Cancer 1997;4:29–32.
8. Akashi-Tanaka S, Fukutomi T, Miyakawa K, Uchiyama N, Tsuda H. Diagnostic value of contrast-enhanced computed tomography for diagnosing the intraductal component of breast cancer. Breast Cancer Res Treat 1998;49:79–86.
9. Healey EA, Osteen RT, Schnitt SJ, Gelman R, Stomper PC, Connolly JL, Harris JR. Can the clinical and mammographic findings at presentation predict the presence of an intensive intraductal component in early stage breast cancer. Int J Radiat Oncol Biol Phys 1989;17: 1217–1221.
10. Tsunoda HS, Ueno E, Tohno E, Akisada M. Echogram of ductal spreading of breast carcinoma. Jpn J Med Ultrasonics 1990;17:44–48 (in Japanese with English abstract).
11. The Japanese Breast Cancer Society. General Rules for Clinical and Pathological Recording of Breast Cancer. Tokyo: Kanehara; 1998. pp 69–72.
12. Lluch A, Cervantes A, Pardo JD, Cervera V, Pallardo Y, Ferrando F, Juan O, Martinez-Agullo A, Azagra P, Lledo S. Assessment of primary tumor and axillary (AX) involvement in breast cancer after neoadjuvant chemotherapy: A comparison of clinical examination, mammography, ultrasonography and CT-scan. Proc Am Soc Clin Oncol 1995;14:135.
13. Mumtaz H, Davidson T, Spitttle M, Tobias J, Craggs MAH, Cowley G, Taylor I. Breast surgery after neoadjuvant treatment. Is it necessary? Eur J Surg Oncol 1996;22:335–341.
14. Gilles R, Guinebretiere J-M, Toussaint C, Spielman M, Rietjens M, Petit J-Y, Contesso G, Masselot J, Vael D. Locally advanced breast cancer: Contrast-enhanced subtraction MR imaging of response to preoperative chemotherapy. Radiology 1994;191:633–638.
15. Trecate G, Ceglia E, Stabile F, Tesoro-Tess JD, Mariani G, Zambetti M, Musumeci R. Locally advanced breast cancer treated with primary chemotherapy: comparison between magnetic resonance imaging and pathologic evaluation of residual disease. Tumori 1999;85:220–228.
16. Tsuboi N, Ogawa Y, Inomata T, Yoshida D, Yoshida S, Moriki T, Kumon M. Changes in the findings of dynamic MRI by preoperative CAF chemotherapy for patients with breast cancer of stage II and III: pathologic correlation. Oncology 1999;6:727–732.
17. Adler DD, Wahl RL. New methods for imaging the breast: techniques, findings, and potential. Am J Radiol 1995;164:19–30.
18. Akashi-Tanaka S, Fukutomi T, Miyakawa K, Nanasawa T, Matsuo K, Hasegawa T, Tsuda H. Constrast-enhanced computed tomography diagnosing the intraductal component and small invasive foci of breast cancer. Breast Cancer (in press).
19. Wahl R, Zasadny K, Helvie M, Hutchins G, Weber B, Cody R. Metabolic monitoring of breast cancer chemohormotherapy using positron emission tomography: initial evaluation. J Clin Oncol 1993;11:2101–2111.
20. Buadu L, Murakami J, Murayama S, Hashiguchi N, Sakai S, Masuda K, Toyoashima S, Kuroki S, Ohno S. Breast lesions: correlation of contrast medium enhancement patterns on MR images with histopathologic findings and tumor angiogenesis. Radiology 1996;200: 639–649.

Jpn J Clin Oncol 2002;32(5)157–161

Original Articles

Accuracy in Estimating Tumor Extension According to Mammographic Subtypes in Patients with Ductal Carcinoma *In Situ*

Masahiko Sato[1], Takashi Fukutomi[1], Sadako Akashi-Tanaka[1], Kunihisa Miyakawa[2], Natsuko Yamamoto[2] and Tadashi Hasegawa[3]

[1]Breast Surgery Division and [2]Diagnostic Radiology Division, National Cancer Center Hospital and [3]Pathology Division, National Cancer Center Research Institute, Tokyo, Japan

Received September 5, 2001; accepted February 13, 2002

Background: The association between subtypes of mammographic findings and histopathological tumor extension in patients with ductal carcinoma *in situ* has remained unclear. The purpose of this study was to investigate the relationship between tumor extension on mammography, by stratifying four subtypes, and histopathological tumor size in patients with ductal carcinoma *in situ*.

Methods: This study was performed on 109 breasts with ductal carcinoma *in situ*. They were treated by mastectomy at our Hospital between January 1990 and December 1999. Findings on mammography were categorized as microcalcification type, spiculated type, circumscribed type or fibrocystic-change type. The microcalcification type consisted of breasts with malignant microcalcifications, regardless of the presence or absence of tumor shadow. We analyzed the relationship between tumor size on mammography in each category and histopathological tumor size. In the breasts with palpable tumors, we compared palpated tumor size and histopathological tumor size according to the mammographic subtypes.

Results: There was no statistical difference between mammographic tumor size and histopathological tumor size for each mammographic subtype (microcalcification type, $P = 0.60$; spiculated type, $P = 0.72$; circumscribed type, $P = 0.055$). The size of the ductal carcinoma *in situ* in microcalcification and spiculated type was estimated approximately by mammography. However, mammography tended to overestimate the circumscribed type. In the cases of palpable tumor, we statistically underestimated the size of ductal carcinoma *in situ* by palpation in microcalcification and fibrocystic-change type (microcalcification type, $P = 0.0001$; fibrocystic-change type, $P = 0.040$).

Conclusion: Mammographic categorization is useful for surgical planning of ductal carcinoma *in situ*, particularly when considering breast-conserving surgery.

Key words: ductal carcinoma in situ – mammography – breast-conserving surgery – microcalcification

INTRODUCTION

The use of screening mammography (MMG) in the United States has resulted in a significant increase in the rate of detection of ductal carcinoma *in situ* (DCIS) from 5% to 25–30% (1,2). The introduction of screening MMG will lead to increased detection of asymptomatic and impalpable DCIS in Japan (3). Breast-conserving surgery for DCIS is gaining acceptance (4,5). The main problem with breast-conserving surgery is local recurrence. Price et al. reported that up to 30% of patients develop recurrent disease following breast-conserving surgery for DCIS within 15 years and, of these, about 50% will have invasive cancer (6). Complete excision with clear margins was associated with a lower tumor recurrence rate (7–9). Margin width is an important factor in predicting the risk of local recurrence following breast-conserving surgery (10–14).

MMG will play an important role in the evaluation of DCIS, and also its detection. The assessment of tumor extension obtained by MMG may assist in the selection of patients for

For reprints and all correspondence: Takashi Fukutomi, Breast Surgery Division, National Cancer Center Hospital, 1–1, Tsukiji 5-chome, Chuo-ku, Tokyo 104-0045, Japan. E-mail: tfukutom@gan2.ncc.go.jp

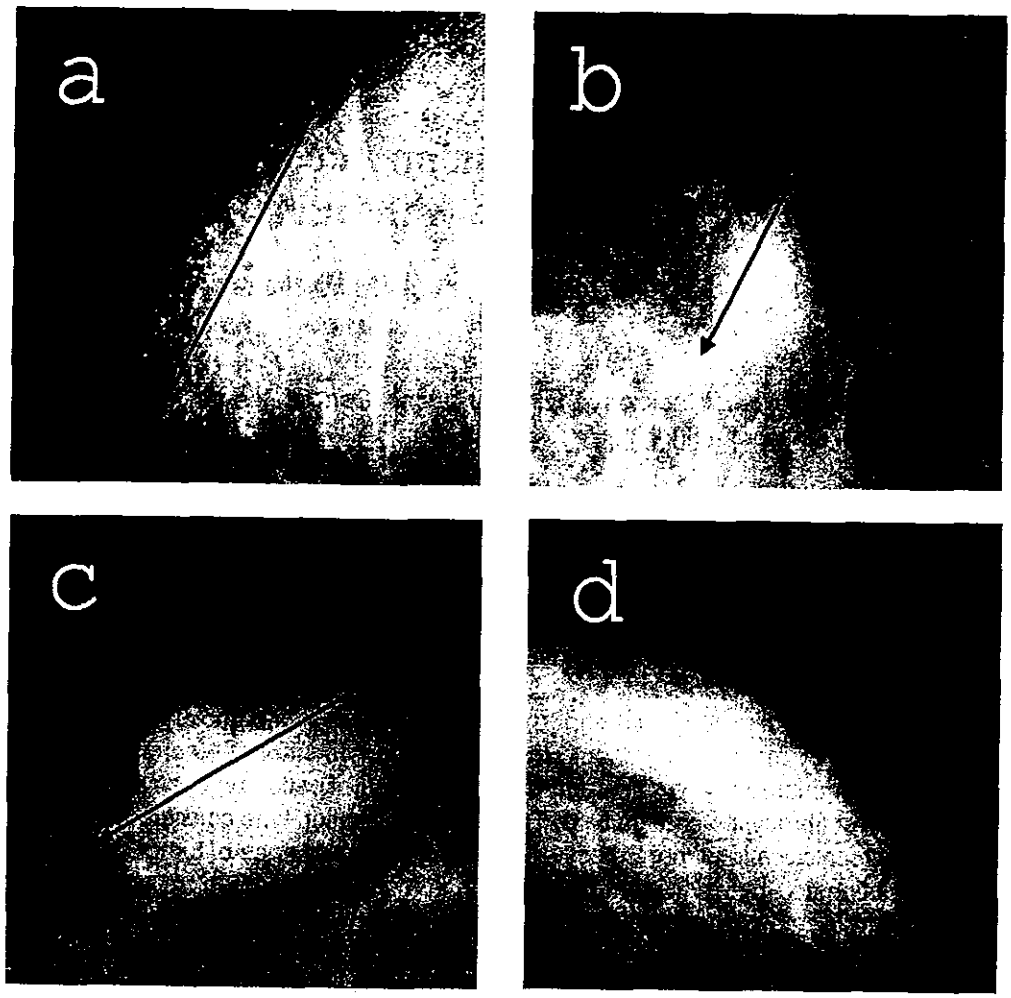

Figure 1. Typical appearances of each mammographic subtype. The lines between arrows indicate the measurement of mammographic tumor extension in each subtype. However in fibrocystic-change type, it is impossible to estimate the tumor extension. (a) Microcalcification type. A mediolateral view of the breast shows linear and coarse granular microcalcifications. (b) Spiculated type. A craniocaudal mammography shows an ill-defined and spiculated mass. (c) Circumscribed type. A craniocaudal mammography shows a well-defined circumscribed mass. (d) Fibrocystic-change type. A spot view of a palpable tumor shows dense tissue. However, there is no recognizable tumor.

breast-conserving surgery and guide the appropriate extent of excision. Holland and co-workers analyzed the association between microcalcification and histopathological tumor extension (15,16), but there is nothing in the literature regarding the association in other MMG subtypes. There are some reports of association in the less common MMG findings of breast malignancy (17,18) and breasts with DCIS (19). The association between subtypes of MMG findings and histopathological tumor extension has remained unclear, particularly in patients with DCIS. In this study, we investigated the relationship between MMG tumor extension and histopathological tumor size according to the MMG subtype. In addition, we compared palpated tumor size with histopathological tumor size according to the MMG subtype in DCIS with palpable tumor.

PATIENTS AND METHODS

Between January 1990 and December 1999, 2757 operations for breast cancer, including 150 breasts with DCIS, were performed at the National Cancer Center Hospital, Tokyo, Japan. There were two radical mastectomies, 117 modified radical mastectomies, 10 simple mastectomies, one total glandectomy and 20 involving breast-conserving surgery. The medical records and pathology reports of 130 consecutive series of DCIS that were treated by mastectomy or total glandectomy only were reviewed. The following patients were excluded from this analysis: 14 patients who underwent open biopsy at another hospital, two patients with ipsilateral invasive breast cancer, one patient with minute DCIS discovered incidentally when she had a biopsy for a benign tumor and four patients whose records were not adequate for analysis. The study population included 107 patients with unilateral DCIS and one with bilateral DCIS for a total of 109 breasts with DCIS in 108 patients.

The procedures for histopathological diagnosis before mastectomy included 32 fine-needle aspiration cytologies, seven nipple discharge cytologies, two core needle biopsies, 43 open biopsies and 22 intraoperative open biopsies. Three mastectomies without prior histopathological diagnosis were carried out.

Table 1. Clinicopathological features classified by mammographic subtype in 109 breasts with ductal carcinoma *in situ*

Mammographic subtype	No. of breasts (%)	Age (years)		Menopausal status		Estrogen receptor status			Predominant histopathological pattern	
		Median	Range	Pre-	Post-	Positive	Negative	Unknown	Comedo	Non-comedo
Microcalcification type	52 (47.7)	49	23–75	32	20	16	13	23	16	36
Spiculated type	23 (21.1)	57	38–80	11	12	13	2	8	4	19
Circumscribed type	11 (10.1)	50	40–75	5	6	7	1	3	1	10
Fibrocystic-change type	23 (21.1)	48	26–80	16	7	6	2	15	4	19
Total	109	49	23–80	64	45	42	18	49	25	84
P value		0.16		0.36		0.099			0.28	

Ninety-three percent of breasts (101 of 109) were symptomatic at referral, 70 had palpable mass, 28 had nipple discharge and three had erosion of nipple. Seven percent of cases (eight of 109) were detected by screening MMG.

The background factors of age, menopausal status, estrogen receptor and predominant histopathological pattern were analyzed. The predominant histopathological pattern of DCIS was categorized as comedo or non-comedo type, including five breasts with intracystic carcinoma.

Mammomat 3 and 3000 (Siemens, Germany) were used for MMG examinations. Mediolateral and craniocaudal MMG views, including spot magnification views, were available for every patient. Radiologists in our hospital evaluated the MMG findings preoperatively, which were categorized as either microcalcification, spiculated, circumscribed or fibrocystic-change type.

The microcalcification type consisted of breasts with apparently malignant clustered microcalcifications, regardless of the presence or absence of tumor shadow. Malignant-appearing microcalcifications were defined as numerous fine, linear or pleomorphic microcalcifications showing a linear or clustered distribution. The spiculated type consisted of breasts with spiculated or ill-defined tumor shadows. The circumscribed type consisted of breasts with circumscribed tumor shadows, suggesting a benign tumor. The fibrocystic-change type consisted of a dense and nodular parenchymal shadow, suggesting fibrocystic disease or no abnormal finding on MMG. Indirect signs, including a single dilated duct or asymmetry of breast tissue, were categorized in the fibrocystic-change type.

The last two subtypes were diagnosed as no malignancy by MMG prior to histopathological examination.

Typical cases of these subtypes are shown in Fig. 1.

We analyzed the relationship between the MMG and histopathological tumor size by stratifying each category. MMG tumor size was defined as the largest diameter of the tumor measured with sliding calipers and was recorded preoperatively. In cases with microcalcification type, the longest distance between microcalcifications on MMG was used as the MMG tumor size. In fibrocystic-change type cases, MMG tumor size could not be measured and was excluded from this evaluation.

The entire surgical specimens taken by mastectomy were sectioned transversely to 10 mm thickness. Histopathological tumor size was measured under a microscope on the individual cross-section. If open biopsy had been performed before mastectomy, the orientation of the biopsy specimen was reported to the pathologist, the specimen was reconstructed and then the size of lesion was calculated.

In only one breast with distinct multiple tumors was the largest MMG tumor size compared with the largest histopathological tumor size. The discrepancy between MMG tumor size and histopathological tumor size was analyzed according to each MMG subtype.

There were 88 breasts (80.7%) with palpable tumors. In the breasts with palpable tumors, we compared palpated tumor size and histopathological tumor size according to each MMG subtype. Fibrocystic-change type DCIS was included in this evaluation.

The background factor of age was analyzed by the Kruskal–Wallis test. The chi-squared test was used to determine the statistical significance between the background factors of menopausal status, estrogen receptor status and predominant histopathological pattern. The relationship among MMG tumor size, palpated tumor size and histopathological tumor size was analyzed statistically by a paired *t*-test. The differences in tumor size between histopathology and MMG in terms of background factors were assessed with Student's *t*-test. Differences were regarded as statistically significant when the *P* value was <0.05. Statistical analysis was performed using Statview version 5.0 (SAS Institute, Cary, NC).

Table 2. Mammographic and histopathological tumor size according to mammographic subtype in 109 breasts with ductal carcinoma *in situ*

Mammographic subtype	Mammographic tumor size (mm)*	Histopathological tumor size (mm)*	*P* Value
Microcalcification type	32.7 ± 22.2	34.2 ± 17.2	0.60
Spiculated type	26.0 ± 10.9	27.3 ± 16.0	0.72
Circumscribed type	34.3 ± 19.7	23.9 ± 10.3	0.055
Fibrocystic-change type	–	29.1 ± 16.7	–

*Mean ± SD.

Table 3. Number, palpated and histopathological tumor size in 88 breasts with palpable tumors according to mammographic subtype

Mammographic subtype	No. of palpable tumors/all (%)	Palpated tumor size (mm)*	Histopathological tumor size (mm)*	*P* Value
Microcalcification type	40/52 (76.9)	23.9 ± 9.3	35.3 ± 18.1	0.0001
Spiculated type	21/23 (91.3)	25.9 ± 9.3	26.9 ± 15.0	0.76
Circumscribed type	11/11 (100)	30.6 ± 15.4	23.9 ± 10.3	0.078
Fibrocystic-change type	16/23 (69.6)	23.4 ± 12.7	31.3 ± 13.5	0.040

*Mean ± SD.

RESULTS

The clinicopathological background factors classified by MMG subtypes are shown in Table 1. There was no significant difference in terms of age, menopausal status, predominant histopathological pattern and estrogen receptor status in each MMG subtype. In the five breasts with non-invasive intracystic carcinoma, four were categorized as circumscribed type by MMG and one breast was of spiculated type. The predominant histopathological pattern of non-invasive intracystic carcinoma was the non-comedo type.

MMG tumor size and histopathological tumor size according to MMG subtypes are shown in Table 2. There was no statistical difference between MMG tumor size and histopathological tumor size in microcalcification and spiculated type (microcalcification type, $P = 0.60$; spiculated type, $P = 0.72$). MMG tended to overestimate the tumor size in the circumscribed type with marginal significance ($P = 0.055$).

The number, palpated and histopathological tumor size in 88 breasts according to MMG subtype are shown in Table 3. In the microcalcification and fibrocystic-change type, histopathological tumor size was significantly larger than palpated tumor size. In the circumscribed type, histopathological tumor size was smaller than palpated tumor size with marginal significance ($P = 0.078$).

The length of MMG tumor size minus histopathological tumor size according to MMG subtype in 86 breasts excluding fibrocystic-change type is shown in Fig. 2. Most breasts (about 70%) were estimated with a discrepancy within 20 mm in each subtype. In the circumscribed type, no breast was underestimated more than 20 mm.

The length of MMG tumor size minus histopathological tumor size according to MMG subtype was compared, with the exception of the fibrocystic-change type, stratified by background factors including age (<50/≥50 years) ($P = 0.98$), menopausal status (premenopausal/postmenopausal) ($P = 0.91$), predominant histopathological pattern (comedo/non-comedo) ($P = 0.59$) and estrogen receptor status (positive/negative) ($P = 0.91$). There was no significant difference among these factors.

DISCUSSION

Mammographically detected microcalcifications were observed in 62–98% of DCIS (19–21). In this study, 47.7% of cases were categorized as microcalcification type. The proportion of microcalcification type was smaller than in the literature. The disparity in the proportion of the microcalcification type can be attributed to patient selection, because patients who underwent breast-conserving surgery were excluded from this study and most of our patients (93%) had clinical complaints initially.

Holland et al. reported that MMG estimates of tumor size, based on the extent of microcalcification, frequently underestimated the histopathological tumor size in cases with DCIS (15). However, the data were inconsistent with our results.

The extent of the discrepancy was partly related to the histopathological pattern of DCIS, especially in predominant non-comedo type, associated with fine-granular microcalcification (15,20,22), which tended to be underestimated more than the comedo type (15). Magnification views are useful for detection of fine-granular microcalcifications (16). A discrepancy between MMG and histopathological size <2 cm was seen in 80–85% of cases, irrespective of the histopathological pattern, when a magnified view was applied (16). In the present study, we confirmed this tendency; a discrepancy between MMG and histopathological tumor size within 2 cm was seen in 76.9% of microcalcification type breasts. Since we used a magnified

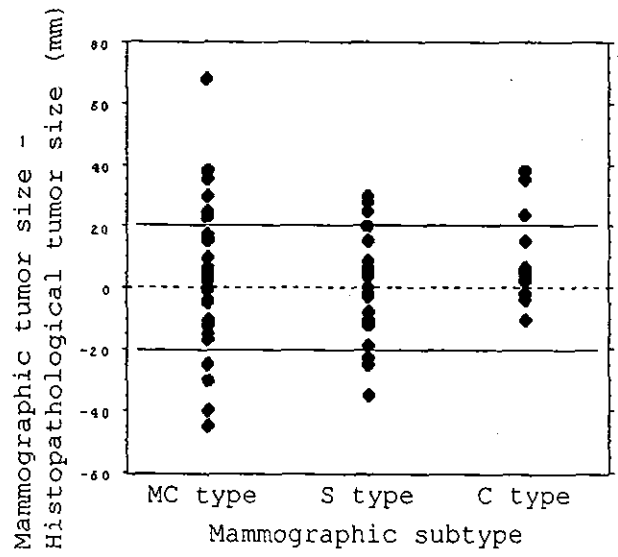

Figure 2. Length of MMG tumor size minus histopathological tumor size according to MMG subtype in 86 breasts, excluding fibrocystic-change type.

view for every breast in this study, MMG adequately evaluated the tumor size irrespective of histopathological pattern. Computed tomography and/or magnetic resonance imaging precisely describe cancerous extension (23). Using these new diagnostic images, patients with microcalcification type can be candidates for breast-conserving surgery.

With regard to the palpable tumor size, it was significantly smaller than the histopathological tumor size in microcalcification and fibrocystic-change type; only for the spiculated type did palpation appropriately estimate tumor size. We therefore estimated the tumor extension adequately by both MMG and palpation in the spiculated type.

In the circumscribed type, MMG and palpation tended to overestimate the tumor size in the present study. Voogd et al. reported that the proportion of patients with non-circumscribed tumors on MMG who had undergone re-excision after an initial biopsy was significantly higher compared with circumscribed tumors, although this study focused on invasive breast cancer (24). The circumscribed type may have a lower risk of leaving a residual tumor when breast-conserving surgery is performed. Most intracystic carcinomas classified as the circumscribed type may exacerbate the increasing frequency of overestimation by MMG.

In the fibrocystic-change type, we could not estimate the tumor extent accurately by MMG, but all patients had clinical symptoms. The tumor sizes of 16 of 23 breasts (70%) were estimated by palpation. However, the histopathological tumor size was significantly underestimated by palpation only ($P = 0.040$). One should therefore be careful when performing breast-conserving surgery for the fibrocystic-change type.

In conclusion, MMG categorization is useful for surgical planning of DCIS, particularly when considering breast-conserving surgery.

References

1. Schwartz GF, Solin LJ, Olivotto IA, Ernster VL, Pressman PI. The consensus conference on the treatment of *in situ* ductal carcinoma of the breast, April 22–25, 1999. *Hum Pathol* 2000;31:131–9.
2. Fryberg E, Bland K. *In situ* breast carcinoma. *Adv Surg* 1993;26:29–72.
3. Morimoto T, Sasa M, Yamaguchi T, Harada K, Sagara Y. High detection rate of breast cancer by mass screening using mammography in Japan. *Jpn J Cancer Res* 1994;85:1193–5.
4. Fisher B, Dignam J, Wolmark N, Mamounas E, Costantino J, Poller W, et al. Lumpectomy and radiation therapy for treatment of intraductal breast cancer: findings from National Surgical Adjuvant Breast and Bowel Project B-17. *J Clin Oncol* 1998;16:441–52.
5. Solin LJ, Recht A, Fourquet A, Kurtz J, Kuske R, McNeese M, et al. Ten-years results of breast conserving surgery and definitive irradiation for intraductal carcinoma (ductal carcinoma *in situ*) of the breast. *Cancer* 1991;68:2337–44.
6. Price P, Sinnet HD, Gusterson B, Walsh G, A'Hern RP, McKinna JA. Duct carcinoma *in situ*: predictors of local recurrence and progression in patients treated by surgery alone. *Br J Cancer* 1990;61:869–72.
7. Fisher B, Dignam J, Wolmark N, Wickerham DL, Fisher ER, Mamounas E, et al. Tamoxifen in treatment of intraductal breast cancer: National Surgical Adjuvant Breast and Bowel Project B-24 randomized controlled trial. *Lancet* 1999;353:1993–2000.
8. Fisher B. National Surgical Adjuvant Breast and Bowel Project breast cancer prevention trial: a reflective commentary. *J Clin Oncol* 1999;17:1632–9.
9. Chan KC, Knox WF, Sinha G, Gandhi A, Barr L, Baildam AD, et al. Extent of excision margin width required in breast conserving surgery for ductal carcinoma *in situ*. *Cancer* 2001;91:9–16.
10. Holland PA, Gandhi A, Knox WF, Wilson M, Baildam AD, Bundred NJ. The importance of complete excision in the prevention of local recurrence of ductal carcinoma *in situ*. *Br J Cancer* 1998;77:110–4.
11. Silverstein MJ, Lagios MD, Martino S, Lewinsky BS, Craig PH, Beron PJ, et al. Outcome after invasive local recurrence of ductal carcinoma *in situ* of the breast. *J Clin Oncol* 1998;16:1367–73.
12. Silverstein MJ. Ductal carcinoma *in situ* of the breast. *Br J Surg* 1997;84:145–6.
13. Holland PA, Knox WF, Potten CS, Howell A, Anderson E, Baildam AD, et al. Assessment of hormone dependence of comedo ductal carcinoma *in situ* of the breast. *J Natl Cancer Inst* 1997;89:1059–65.
14. Cheng L, Al-Kaisi NK, Gordon NH, Liu AY, Gebrail F, Shenk RR. Relationship between the size and margin status of ductal carcinoma *in situ* of the breast and residual disease. *J Natl Cancer Inst* 1997;89:1356–60.
15. Holland R, Hendriks JH, Verbeek AL, Mravunac M, Shuurmans Stekhoven JH. Extent, distribution and mammographic/histological correlations of breast ductal carcinoma *in situ*. *Lancet* 1990;335:519–22.
16. Holland R, Hendriks JH. Microcalcification associated with ductal carcinoma *in situ*: mammographic–pathologic correlation. *Semin Diagn Pathol* 1994;11:181–92.
17. Sickles EA. Mammographic features of 'early' breast cancer. *Am J Roentgenol* 1984;143:461–4.
18. Ciatto S, Cataliotti L, Distante V. Nonpalpable lesions detected with mammography: review of 512 consecutive cases. *Radiology* 1987;165:99–102.
19. Ikeda DM, Anderson I. Ductal carcinoma *in situ*: atypical mammographic appearances. *Radiology* 1989;172:661–6.
20. Stomper PC, Connolly JL, Meyer JE, Harris JR. Clinically occult ductal carcinoma *in situ* detected with mammography: analysis of 100 cases with radiologic–pathologic correlation. *Radiology* 1989;172:235–41.
21. Evans A, Pinder S, Wilson R, Sibbering M, Poller D, Elston C, et al. Ductal carcinoma *in situ* of the breast: correlation between mammographic and pathologic findings. *Am J Roentgenol* 1994;162:1307–11.
22. Stomper PC, Connolly JL. Ductal carcinoma *in situ* of the breast: correlation between mammographic calcification and tumor subtype. *Am J Roentgenol* 1992;159:483–5.
23. Akashi-Tanaka S, Fukutomi T, Miyakawa K, Uchiyama N, Tsuda H. Diagnostic value of contrast-enhanced computed tomography for diagnosing the intraductal component of breast cancer. *Breast Cancer Res Treat* 1998;49:79–86.
24. Voogd AC, van der Horst F, Crommelin MA, Peterse JL, van Beek MW, Repelaer Driel OJ, et al. The relationship between findings on pre-treatment mammograms and local recurrence after breast-conserving therapy for invasive breast cancer. *Eur J Surg Oncol* 1999;25:273–9.

Breast Cancer
Vol. 10 No. 3 July 2003

Review Article

The Role of Computed Tomography in the Selection of Breast Cancer Treatment

Sadako Akashi-Tanaka*[1], Takashi Fukutomi*[1], Natsuko Sato*[2], and Kunihisa Miyakawa*[2]

*[1]*Division of Breast Surgery, and* *[2]*Department of Diagnostic Radiology, National Cancer Center Hospital, Japan.*

Contrast-enhanced computed tomography (CE-CT) is one of the most sensitive imaging modalities. CE-CT plays a role in the following: (1) to determine the extent of breast cancer to select the appropriate breast conserving treatment (BCT). The sensitivity and specificity for the detection of extensive intraductal component (EIC) by CE-CT were 82-88% and 75-89%, respectively. The pathological extent of tumors significantly correlated with the extension revealed by CE-CT; (2) to determine the extent of resection following neoadjuvant chemotherapy, which is difficult to assess by other modalities; (3) to diagnose axillary lymph node metastasis. The sensitivity and specificity are 79-90% and 70-89%, respectively; (4) to identify occult breast cancer with axillary metastasis and to diagnose local recurrence after BCT.

Breast Cancer 10:198-203, 2003.

Key words: Breast cancer, CT scan, Breast conserving Treatment, Neoadjuvant chemotherapy, Axillary lymph node

Contrast-enhanced computed tomography (CE-CT) is one of the most sensitive imaging modalities to supplement mammography (MMG) and ultrasonography (US). The ability of CT to distinguish benign from malignant tumors has been evaluated. However, considering its high spatial resolution and relatively low specificity, CE-CT is adequate for evaluating tumor extension within the breast and detecting small lesions not visualized by other methods. Helical CT technology reduces X-ray exposure compared to conventional CT and enables a more rapid scan without gaps[1]. The advent of multidetector-row CT (MD-CT), enabling high spatial resolution with more rapid scanning than helical CT, will widen the role of CT in breast cancer management.

Reprint requests to Sadako Akashi-Tanaka, Division of Breast Surgery, National Cancer Center Hospital, 5-1-1 Tsukiji, Chuo-ku, Tokyo 104-0045, Japan.
E-mail: sakashi@gan2.ncc.go.jp

Abbreviations:
CE-CT, Contrast-enhanced computed tomography; MMG, Mammography; US, Ultrasonography; MD-CT, Multidetector-row computed tomography; BCT, Breast conserving treatment; EIC, Extensive intraductal component; 3D, 3-Dimensional; NAC, Neoadjuvant chemotherapy; SLN, Sentinel lymph node; CE, Clinical examination

Received April 4, 2002; accepted May 9, 2002

Determining the Extent of Breast Cancer and Selecting Optimal Candidates for Breast-Conserving Treatment

Currently, women with early breast cancer have a choice among local therapy, mastectomy or breast conserving treatment (BCT). To select optimal candidates for BCT, preoperative assessment of tumor extension including extensive intraductal component (EIC), multicentricity and daughter lesions in the same breast is essential[2]. Resection margins that are clear of tumor are associated with the best local control for patients who choose BCT[3]. Multiple reexcisions and the accompanying anxiety could be reduced if we had better methods of defining the tumor extent before surgery. Microcalcifications on MMG[4] and dilated ducts on US[5] are typical findings of EIC, but MMG and US are of little value in cases without these findings. The sensitivity of MMG for detecting EIC has been reported to be 41%-81%. Multicentricity is often undetected by MMG[4-6].

CE-CT can provide this information. Studies using CE-CT for this purpose have been reported mostly from Japan[7-15]. Almost all invasive malignancies are enhanced with non-ionic iodine contrast material, and malignancies may show much more rapid initial enhancement than benign lesions. The delay between initiation of bolus injection at a rate of 2 ml/s and scanning was 40-60 seconds[7-9],

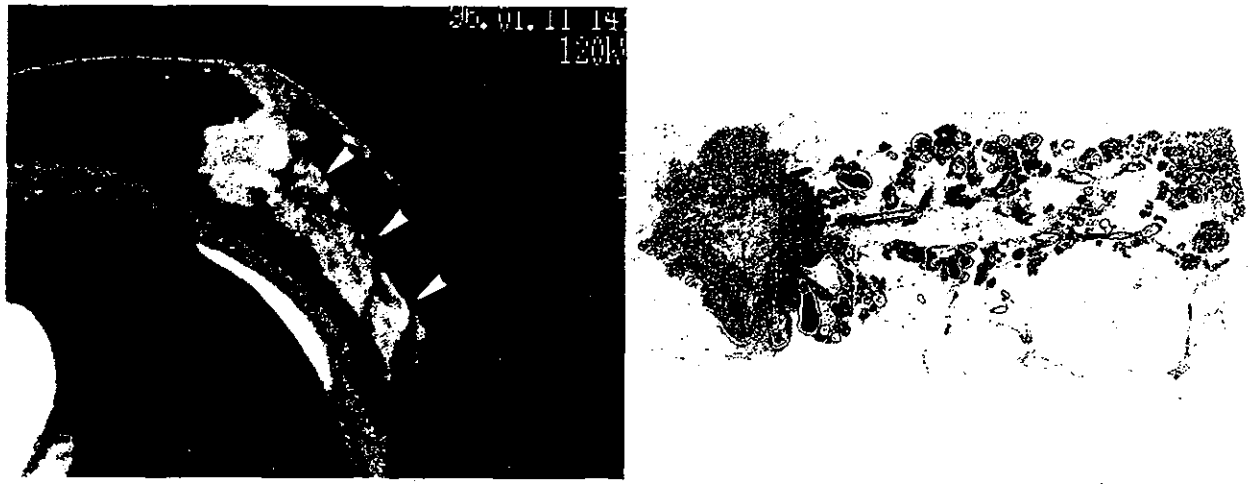

Fig 1. (a) An example of tumor and spotty (arrow) enhancement on CE-CT. (b) Low magnification of the resected specimen. Tumor extension including EIC correlated with CE-CT findings.

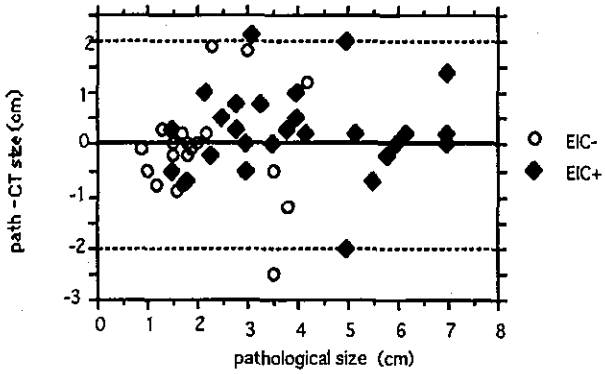

Fig 2. Differences between the size of tumor extension estimated by CE-CT and the pathological extent[10].

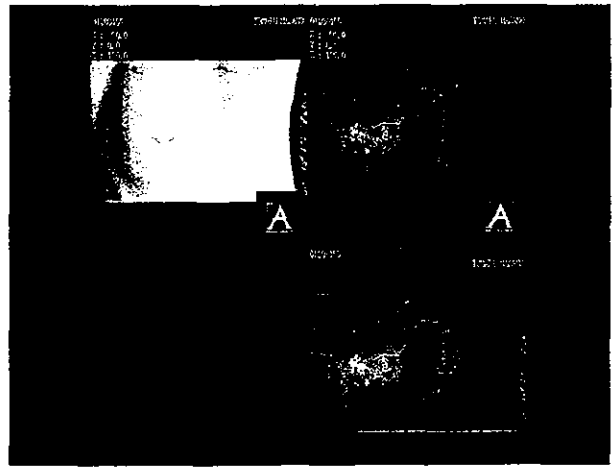

Fig 3. 3D image of non-palpable breast cancer presenting with nipple discharge (right lower) by superimposing surface rendering images (left upper) and volume rendering images (right upper).

or a 70-100 second delay with a 1.5 ml/s injection[10]. When spotty nodular or linear enhancements are demonstrated more than 10 mm beyond the index tumor on CE-CT, EIC and small invasive foci such as multicentricity and daughter lesions are defined as positive[7-10] (Fig 1). The sensitivity, specificity and accuracy for detecting EIC were 82~88%, 75~89% and 75~83%, respectively[10-14]. Using MD-CT, the sensitivity and specificity for the detection of EIC were 80% and 100%, respectively[15]. The pathological extent of tumors significantly correlates with the extension revealed by CE-CT[10]. The correlation between CE-CT and histologic assessment of tumor extent is shown in Fig 2[11]. The main causes of false positive detection of EIC were ductal hyperplasia, papillomatosis, sclerosing adenosis and intraductal papilloma[10, 11]. On the contrary, non-comedo type intraductal spread and lobular carcinoma *in situ* could be the causes of false negative results[11]. Ishida and Hisamatsu compared the accuracy of MRI and CE-CT for detecting EIC and multicentricity. They have almost equivalent accuracy but MRI demonstrated slightly better sensitivity and worse specificity[16, 17]. The advantage of CT over MRI is that CE-CT breast images are obtained with patients in the supine position used during surgery, thus providing precise information about the tumor extent (Fig 3); in contrast, in most previous studies of MRI, patients were examined while prone to minimize motion of the breast during breathing.

Determining the Extent of Resection after Neoadjuvant Chemotherapy

Neoadjuvant chemotherapy (NAC) for operable breast cancer has recently become widely accepted. The results of the NSABP B18 study

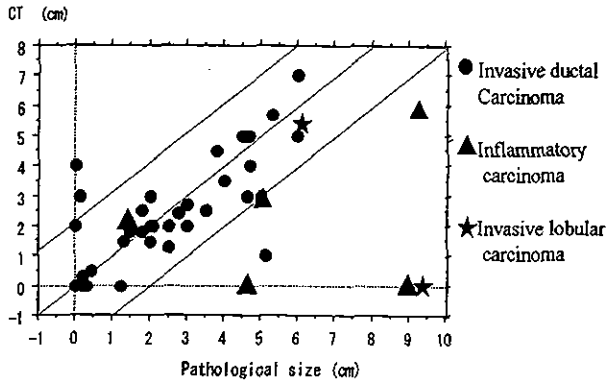

Fig 4. Correlation between sizes determined by CE-CT and pathological measurements[20].

confirmed that there was no differences in survival between patients treated with either neoadjuvant or adjuvant therapy when using the same regimen before or after surgery[18]. NAC reduced tumor size and allowed BCT in patients who would otherwise be treated with mastectomy. NAC also plays a role as an *in vivo* chemosensitivity test. However, after NAC, there are problems in the management of breast cancer related to defining the extent of residual disease. Clinical measurements of breast masses are often inaccurate, and there are substantial interobserver variations among examiners[19]. An increased rate of breast recurrence was noted in down-staged patients who were initially eligible for mastectomy (14.5%) compared with patients who were already candidates for BCT before NAC (6.9%) in the NSABP study[18]. This suggests that a more accurate modality for evaluating residual tumor is needed.

We evaluated the accuracy of diagnostic images for demonstrating the extent of residual tumor following NAC administration[20]. The discrepancy between tumor extension determined by CE-CT and pathologically was less than 2 cm in most cases (92%) (Fig 4). CE-CT demonstrated the extent of the residual cancerous lesions following NAC administration more accurately than other conventional diagnostic methods, such as MMG and US (Fig 5). However, inflammatory breast cancer and invasive lobular carcinoma should be treated carefully because they are not accurately visualized by CE-CT.

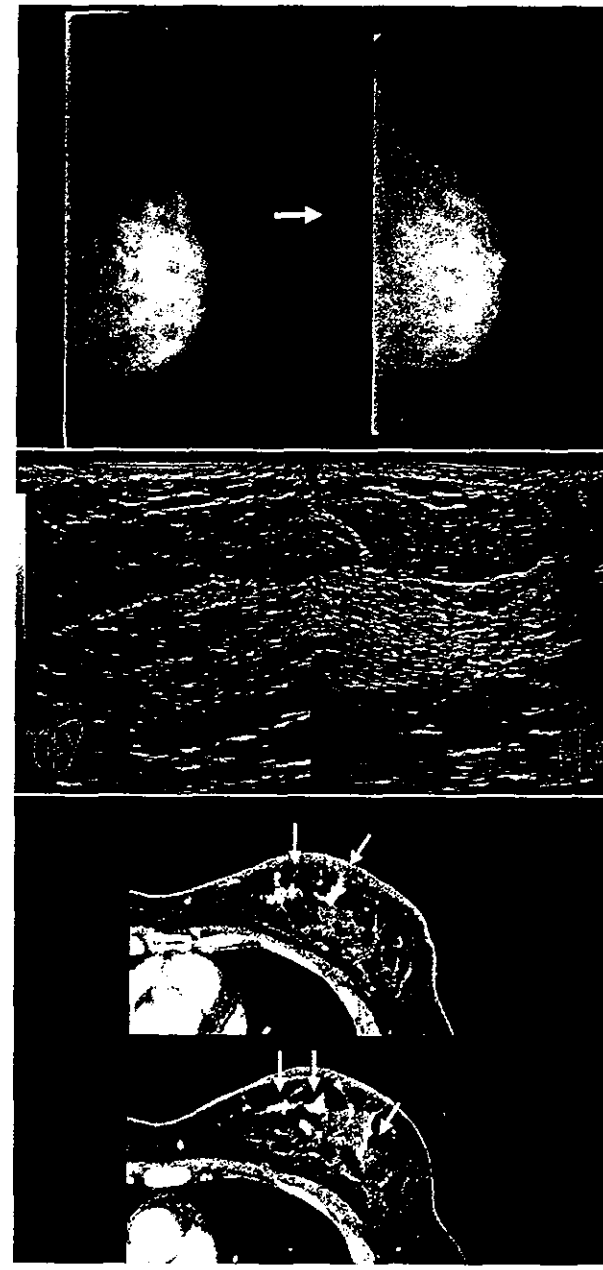

Fig 5. (a) MMG findings before (left) and after (right) NAC administration. (b) Almost normal findings by US after NAC administration. (c) Spotty enhancements (arrow) on CE-CT were visualized in almost the whole breast after NAC administration. Scattered invasive ductal carcinoma remained (6.5 × 3.5 cm) in the surgical specimen.

Diagnosis of Axillary Lymph Node Metastasis -Axillary Dissection or Sentinel Node Biopsy?-

Axillary lymph node dissection has been a standard procedure in the management of breast cancer. However, in a patient with pathologically negative axilla, the necessity of routine dissection is being questioned. A non-invasive method of accurate diagnosis is needed. Sentinel lymph node (SLN) biopsy offers the possibility of reliably identifying patients with axillary node involvement with a low-morbidity operation[21]. It should be emphasized that SLN is an appropriate technique only for patients with clinically negative axillae[22].

Table 1. Accuracy of Detecting Axillary Metastasis by CE-CT

	Nishie[26]	Suzuki[25]		Ogawa[24]	March[23]
Section	3-5 mm	5 mm	3 mm	5 mm	10 mm
Definition of LN metastasis	Enhanced > 1 cm & asymmetry Spicula	Oval or round Iso-density Well demarkated		> 5 mm on short diameter	> 10 mm
	n = 36	n = 211	n = 46	n = 41	n = 20
Sensitivity	81.3%	82.4%	78.9%	90.0%	50%
Specificity	75.0%	70.0%	88.9%	85.7%	75%
Accuracy	77.8%	75.4%	84.8%	87.8%	55%
NPV	83.3%	84.0%	85.7%	90.0%	20%

NPV, Negative predictive value

A lymph node fully occupied by cancer cells may be skipped by lymphatic drainage and cause a false negative SLN. Preoperative diagnosis of negative lymph node metastasis by diagnostic imaging has become important when planning SLN biopsy.

There have been some reports on the diagnosis of axillary lymph node involvement using CT as shown in Table 1. When using 10 mm sections in the early 1990s, CT was not an accurate predictor of axillary LN involvement[23]. With improvements in helical CT technology, the sensitivity and specificity have improved to 79 - 90% and 70 - 89%, respectively[24-26]. The average sensitivity of immunoscintigraphy, Fluorine-18-fluorodeoxy glucose (FDG) PET and SPECT imaging is reported to be 77% with a specificity of 89% for detecting axillary metastases in patients with primary breast cancer[27].

Uematsu *et al.* examined the relationship between the internal structure of small excised lymph nodes and the findings of high resolution helical CT[28]. Abnormal (eccentric or irregular) cortices were observed in malignant nodes ($p < 0.0001$). Nodes with a longest-shortest axis ratio equal to or less than 2 were regarded as highly likely to be malignant.

Nodal status following downstaging remains the major prognostic factor for survival[29]. Patients who received NAC were unlikely to have nodal metastases that could be reliably identified by SLN. Accurate imaging methods to assess axillary involvement after NAC are important. Lluch *et al.* evaluated axillary involvement after NAC in 60 breast cancer patients using clinical examination (CE), US and CT[30]. Sensitivity was 27%, 25% and 68.5% respectively for CE, US and CT. Specificity was 96%, 100% and 73.5% respectively for CE, US and CT. CT was a sensitive and accurate noninvasive technique to assess AX involvement after NAC. 3D images of axillary lymph nodes in patients following NAC using maximum intensity projection (MIP) is shown in Fig 6.

Fig 6. 3D image of axillary lymph node (arrow) processed by MIP after NAC. Nine of 10 dissected lymph nodes were involved by cancer, pathologically.

Specific Application of Breast CT for Occult Breast Cancer with Axillary Metastasis and Follow-up

CT can provide important information for follow-up in women who undergo BCT. It is sensitive for diagnosing local recurrence, even in non-palpable lesions[31]. The sensitivity and specificity for local recurrence is 91% and 85%, respectively.

It is possible to use CE-CT to identify primary